Transactions of the Materials Research Society of Japan 32[1] 203-208 (2007)

Real-time observation of Si and SOI substrates during thermal oxidization

T. Kawamura, H. Omi, S. Fujikawa* and J. Matsui**
NTT Basic Research Laboratories,
3-1, Wakamiya Morinosato, Atsugi, Kanagawa 243-0198, Japan
Fax: +81 46 240 3494, e-mail: kawamura@will.brl.ntt.co.jp
*University of Hyogo, 3-2-1, Koto, Kamigori-cho, Ako-gun, Hyogo 678-1297
**Center for Advanced Science & Technology, 3-1-1, Koto,
Kamigori-cho, Ako-gun, Hyogo 678-1205

Semiconductor devices will soon reach physical limitation and several new technologies have been proposed to overcome it. Among them are silicon-on-insulator (SOI) substrates, which are thought to be ideal substrates since they reduce the body effect and parasitic junction capacitance, which degrade device performance. Additionally, fabricating devices on SOI substrates less than several ten nanometers thick and operating them in the fully depleted mode offers further performance advantages.
Several techniques have been proposed to fabricate SOI substrates, such as oxygen-ion implantation, wafer bonding with a thinning process or hydrogen-ion implantation. The remaining issue is how to improve the crystalline quality of SOI substrates using these techniques. Since the substrates are formed in the thermally equilibrium condition at high temperature, the difference of thermal expansion coefficients induces defects and interface strains during the cooling process. Grazing incidence x-ray diffraction (GIXD) is more sensitive to the internal strains of thin SOI since the penetration depths of x-rays can be controlled by changing incident angles. We have recently succeeded in observing the strain structures of various SOI substrates in real-time using the GIXD technique.
Key words: Si, silicon-on-insulator, grazing incidence x-ray diffraction, thermal strain

1. INTRODUCTION

For 50 years, Si has played important role in the development of the electronic device integration. Although the electrical properties of bulk germanium are better than these of silicon, and the first transistor was invented using Ge crystals [1], the electronics industry have been using Si materials for device applications because Si offers one great advantage for device fabrication. The MOSFET transistor structures shown schematically in Fig. 1. There are several factors to consider for improving MOSFET performance. A important one is the smooth flow of electron and hole carriers from the source to the drain without trapping by the interface states. In contrast to the GeO_x and Ge interface, the number of interface states between Si and SiO_2 is very small [2]. This guarantees the smooth flow of carriers and normal device operation when device size and channel length are reduced. The performance improvement of the silicon-based devices stands on this scaling-law. The density of defects at the interface is estimated to be lower than $10^{12}cm^{-2}$, although the number of the dangling bonds of raw Si(001) is about $1.36x10^{15}cm^{-2}$. This means that the 99.9% of defects at the interface are extinguished during the thermal oxidization and the formation of SiO_2/Si interface. Additionally, an atomically flat interface can be formed by oxidization [3-6], which also simplifies the device fabrication process. However, with the recent progress of device fabrication technology, we have reached to the physical limitation of Si and a breakthrough to overcome the physical limitation is urgently needed.

Si substrate formed on an insulator, called silicon-on-insulator (SOI), is attractive as the next-generation substrate because it could help us to overcome the physical limitation of electron devices, which is manifested in the short-channel effect, body effect, and parasitic junction capacitance. The idea of SOI substrates was proposed 20 years ago [7], and progress in fabrication techniques has made it possible to establish electronic devices on SOI substrates. Many fabrication processes have been proposed for SOI substrates, and recently, mainly two, the SIMOX

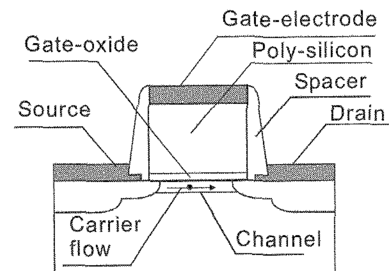

Fig. 1. MOSFET structure.

(Separation by Implanted Oxygen) [7] and Uni-bond [8] techniques, have been used. The SIMOX and Uni-bond techniques are schematically shown in Figs. 2 (a) and (b) respectively.

Although the details of the processes are different, in both an Si layer sandwiched by SiO_2 layers are formed, which is used as the substrate for several transistor circuits after removing an upper oxide layer. Considering the thermal expansion difference between Si and SiO_2 layers and that thermal strains should exist

at the interface, it is surprising that electronic devices on SOI layers work without showing any thermal strain effects. However, future devices on SOI substrates will need thinner SOI layers, for which the influence of the interface imperfectness will increase. Precise structural evaluations of very thin SOI layers and interfaces are therefore required.

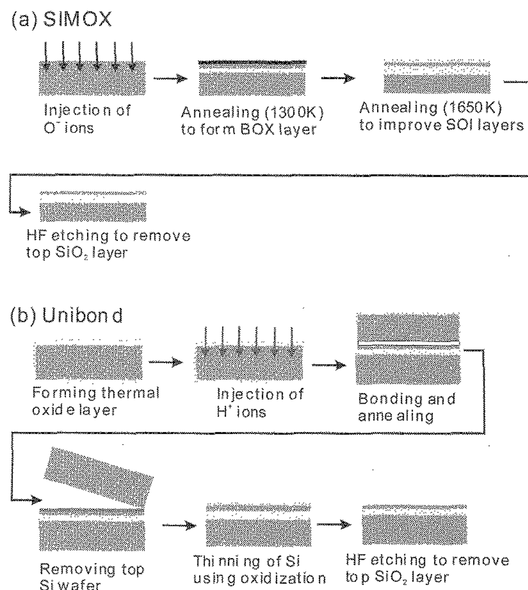

Fig. 2. (a) SIMOX and (b) Uni-bond fabrication processes.

Transmission electron microscopy (TEM) has been traditionally used to observe the internal structure of layered films with atomic resolution. In analyzing the SOI structure, some difficulties arise, such as the release of the strains in the SOI layer during the preparation procedure, and insufficient accuracy for determining absolute strain values. Additionally, TEM observation is done in a vacuum, which makes it difficult to apply TEM to visualize the "real" interface during the thermal oxidization.

Owing to their large penetration ability, x-ray-based techniques have been used to analyze structural changes of materials in solids, liquids, and gaseous environments. The difficulty of the real-time monitoring of the Si thermal-oxidization process mainly arises because of the different requirements for the x-ray measurement and Si oxidization furnace. To solve this problem, we developed a new x-ray diffractometer and furnace system for the Si thermal-oxidization analysis. In this article, we describe the recent understandings we have gained on Si oxidization mechanics and structural changes of SOI substrates using x-ray reflectivity and grazing incidence x-ray diffraction techniques [9].

2. MECHANISM OF SILICON-OXIDIZATION

The mechanism of silicon oxidization has been widely investigated because of its great importance for both surface science and industry applications. In spite of the previous researches on Si oxidization in ultra high vacuum, our understanding of the thermal oxidization is insufficient, owing to the lack of an atomic-scale evaluation tool. Figure 3 shows the schematic drawings of thermally Si oxidization process. When Si substrates are heated in O_2 ambient at 600°C – 1200°C, very smooth and uniform SiO_2 film is formed. If the Si substrates are adequately prepared, an atomically flat interface can be easily obtained by thermal oxidization, which is very important for industrial applications. Deal and Grove [10] introduced the linear-parabolic model, which describes how silicon oxidization occurs at the interface, and this model has been used to explain silicon oxidization in several conditions. The exceptions to this model have been found in the oxidization of very thin (less than 20-nm) silicon-oxide layers, and Massoud et al. [11] has introduced on empirical equation that matches the faster growth rate at the initial oxidization stage, although the physical meaning of this model has not been explained.

The interface structure of SiO_2/Si has been analyzed using several techniques, such as x-ray photoelectron spectroscopy (XPS), Rutherford backscattering spectrometry (RBS), reflectance difference spectroscopy (RDS), medium energy ion scattering (MEIS), electron energy loss spectroscopy (EELS) and x-ray reflectivity (XR) [12-17]. The results have shown that the transition from the SiO_2 to Si bulk crystal is very steep, and there is a transition layer whose density is higher than that of the oxide layer. The high-energy EELS observation [18] suggests that there is a large difference between the transition layer and the bulk amorphous SiO_2 layer, which would mean that the number of second nearest oxygen atoms in the transition layer is smaller than in bulk a-SiO_2 layer. The x-ray reflectivity results have shown a high-density transition layer of about 1-nm thickness [15]. From x-ray scattering measurements, along the [11L] direction [19], a Bragg-like peak was found at (11 0.48), and this structure was firstly assigned

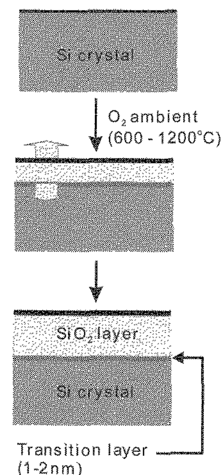

Fig. 3. Si thermal oxidization process.

to the interface transition layer, which is similar to the cristobalite phase. However, a recent energy calculation of large-scale atom models using molecular dynamics [20] has revealed that this peak is caused by the long-range ordering in the oxide layer, which is consistent with the calculation of x-ray scattering. The structure of the transition layer is still uncertain.

3. INSTRUMENTS

For the real-time observation of silicon oxidization, no metals can be used in the furnace since they can be easily oxidized and form several oxide metals that disturb the Si oxidization. Additionally, Si is also reactive with several materials at high temperature, causing the formation of silicon alloys on the substrates and making it difficult to fix silicon substrates on the sample holders. These difficulties limit the design of the goniometer, and we selected a z-axis geometry [21] instead of the normal four-axes one. Figures 4(a) and (b) show the angle parameters for the z-axis geometry and a drawing of the z-axis goniometer. The incident angle μ and reflection angle γ can be varied from 0° to 10° degrees, and 0° to 60° degrees, respectively. The large scanning range of γ by combining θ and δ rotation gives wide scanning range along [00L] without changing the incident angle. Possible ranges of sample rotation θ and detector rotation δ are 0° to 360°, and 0° to 120° degrees, which can cover most of all in-plane diffractions in (HK0) plane. By combining with these angles, one can measure a large (HKL) region in the reciprocal space with constant grazing incidence angles.

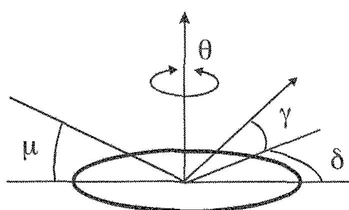

(a) Z-axis geometry

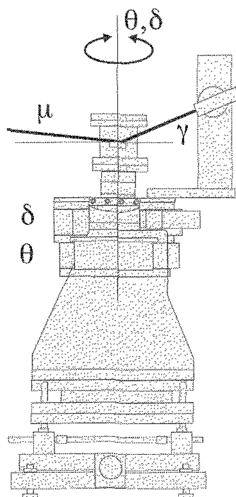

(b) Z-axis goniometor

Fig. 4. (a) Angle parameters for z-axis geometry, and (b) a side view of the z-axis diffractometer.

4. EXPERIMENTAL

All x-ray reflectivity and grazing incidence x-ray diffraction measurements were performed using the z-axis goniometer at the beamline BL24XU of SPring-8 [22]. The 0.124-nm x-ray was collimated to about 1-mm (H) x 0.2-mm (V) using horizontal and vertical slits upstream from the goniometer. To improve the signal to noise ratio, vertical double slits were used for the reflectivity measurement, and a combination of a solar-slit and vertical slit was used for the grazing incidence x-ray diffraction measurement. The incident angles of grazing incidence x-ray diffraction were varied from 0.01^o to 0.4^o.

Si(001) and SOI on Si(001) wafers were used and both the reflectivity and in-plane diffractions at the grazing incidence condition were measured at several temperatures during the oxidization annealing. Additionally, to observe the strain changes in SOI substrates clearly, a SIMOX wafer with (001) surface and a diameter of 15 mm was selected. After the SIMOX wafer had been etched in HF dilute solution, it was oxidized at 1200 °C in a 0.2% O_2/Ar mixture to form a silicon oxide layer on top of the SOI layer and promote the formation of an internal thermal oxide layer on the bottom of the SOI. Then, the thermal oxide on the SOI layer was removed in a HF bath and x-ray diffraction was measured from the 47-nm-thick SOI on top of the SIMOX wafer. It is noted that the density of O_2 was kept constant during all oxidization measurements to simplify the experimental conditions.

5. RESULTS AND DISCUSSIONS

5-1. INTERFACE STRUCTURE OF SiO_2/Si

Figure 5 shows the x-ray reflectivity of a Si(001) wafer measured at 1100 °C, 800 °C, and room temperature after oxidization. Small oscillations were clearly observed, which correspond to the interference of reflected x-rays at the surface and at the SiO_2/Si interface. During the oxidization, the x-ray intensity did not change, suggesting the surface and interface smoothness could be maintained on an atomic scale. After the cooling process, a decrease of the reflectivity intensity and an increase of diffuse scatterings beside the specular reflection were observed, indicating the surface roughening during the cool-down process. Additionally, small changes of the oscillation amplitude were seen with varying substrate temperature, suggesting a different state of the transition layer at each temperature.

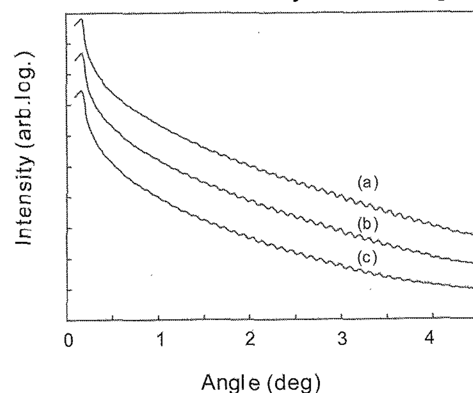

Fig. 5. X-ray reflectivity taken at several substrate temperatures. (a) Ts = 1100°C, (b) Ts = 800°C, and (c) room temperature after oxidization.

To emphasize the oscillation characteristics, the oscillation was extracted using the smoothing technique

[14]. Figure 6 shows the intensity ratio of reflectivity normalized by the smoothed profiles. Enveloped oscillations are clearly observed, and changes in the shape of the envelope and amplitude of the oscillation were observed with varying substrate temperature. Arrows show the estimated anti-node angles of the envelope, which increase at higher temperature. From reflectivity calculations using a simple three-layer model composed of the SiO_2 layer, transition layer, and Si substrate, we found the amplitude of the oscillation is related to the difference in the densities between each medium and that the angle position of anti-nodes corresponds to the thickness of the transition layers. During the oxidization, both the anti-node position and amplitude became larger than at room temperature, and this was more obvious at higher temperature, showing that the average thickness and density of the transition layer during the oxidization are smaller and larger, respectively. Considering that Si oxidization is a layer-by-layer phenomenon and that oxidization speed is higher at higher temperature, the transition layer would be less stable and rapidly changes to the SiO_2 structure at faster oxidization.

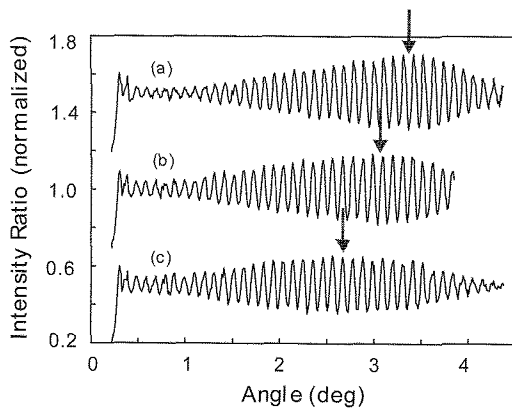

Fig. 6. Oscillation profiles at (a) Ts = 1100°C, (b) Ts = 800°C, and (c) room temperature after the oxidization. Arrows show the anti-node position of each profile.

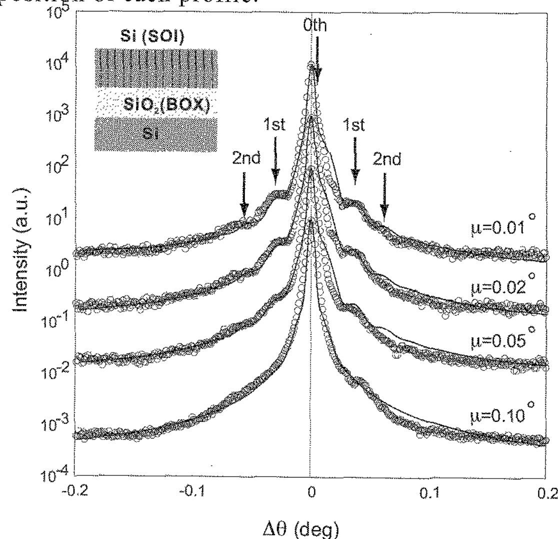

Fig. 7. In-plane Si(220) profiles with various incident angles.

5-2. INTERNAL STRAINS OF THIN SOI LAYERS

Since the lattice constant of SOI substrates is almost same as that of Si substrates and miss-orientation angle of SIMOX wafers is usually very small, it is difficult to obtain strain information from ordinary x-ray diffractions. We therefore used grazing incidence x-ray diffraction at the total-reflection region. Figure 7 shows the measured (220) Bragg diffraction profiles of 47-nm SOI/120-nm SiO_2/Si at different grazing angles from 0.01° to 0.1°. Considering that penetration depth of x-rays in this region is about several nanometers, diffraction would mainly occur in the SOI layer. It should be noted that the Bragg diffraction from the substrate was still observed in the total reflection region, because a part of x-ray could reach the substrate and cause the Bragg diffraction. This explains the strong peak at the center ($\Delta\theta$=0), which comes from the substrate.

Additional oscillating sub-peaks (denoted 0th, 1st, 2nd in the figure) appear at the lower and higher sides of the Si(220) reflection, suggesting the existence of interference domains. These oscillations were clearly observed at incident angles between 0.01° and 0.1° but they merged with the main peak. This suggests that they originate from the surface region of the sample. In addition, it can be seen that the oscillating peaks are asymmetric with respect to the center of the Si(220) peak. The asymmetric feature also became clear when the grazing angle was decreased from 0.1° to 0.01°. These findings indicate that the origin of the peak oscillation is independent of the strong peak related to the bulk Si(220) reflection, suggesting the existence of finite domains at the SOI surface.

The oscillating curves at the side of the main Si(220) peak were analyzed using the framework of the semi-kinematical scattering theory [23]. In this theory, Bragg diffraction is described by the classical Laue-function, but several parameters determined from the dynamical theory, such as the structure factor, dielectric constants, reflective indices, and domain size, are included. This treatment is valid for very thin and strained films where the multiple scatterings of the Bragg diffraction can be ignored. Additionally, the main peak fitted with a Voigt-type function was added, and the intensity ratio between two parts was optimized during the calculations.

To interpret the observed oscillations, we supposed a simple two-layer model (surface region and underlying region in the SOI layer) as the primary approximation, where the surface region is composed of finite domains and the underlying region was treated as the continuous film with large internal strains. We also assume that the distribution of domain size is a Gaussian function, with average size and standard deviation. Considering that the main peak-width was not changed with several incident angles, and the value of peak width is ten times larger than that of Si substrate, the intensity contribution from the substrate can be neglected in the calculations. The solid lines in Fig. 7 are the results of the calculations based on the two-layer model for different angles, and the inset of Fig. 7 shows the schematic model of strained SOI layers. The simulation reproduces well the experimental data, and the obtained strain parameters show that the difference in in-plane strain between the

surface region and the remaining one is a few 10^{-4}. The size of the strain domain in the surface region is about 500 nm with deviation of 70 nm. Table 1 summarizes the strain and domain parameters with various incident angles.

Table 1. Obtained fitting parameters with various incident angles. (α : incident angle, ε : strain value, D: average domain size, σ : deviation of domain size).

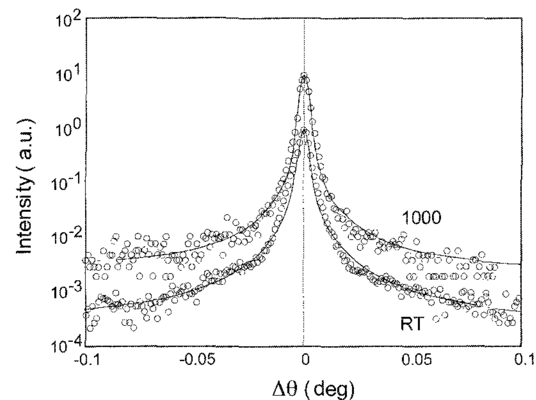

Fig. 8. Si(220) profiles during and after annealing.

The thermal stability of the SOI layer was also investigated using grazing x-ray diffraction. Figure 8 shows the Si (220) profiles taken at 0.01° during annealing at 1000°C and at room temperature. When the sample was annealed at 1000°C, the oscillations on the tail of the main Bragg peak and the asymmetry of the main peak disappeared, suggesting that the strains at the surface region and underlying layer were released and a uniform SOI layer was formed. The Bragg profile at room temperature also shows the same feature, indicating that the post-annealing treatment is effective in improving the spatial inhomogeneous strain distribution in SOI layers.

6. SUMMARY

In summary, we evaluated the transition layer between SiO_2 and Si substrate and internal strains using real-time x-ray reflectivity and grazing incidence x-ray diffraction at the total reflection region.

From the real-time reflectivity analyses, we found that the transition layer is thinner and the density of the layer seems higher at high oxidization temperature, suggesting that the transition layer is less stable and easily changes to the SiO_2 structure during the oxidization. This is consistent with the layer-by-layer oxidization model.

The internal strains of the thin SOI substrate were evaluated using grazing x-ray diffraction at the total reflection region. When the incident angles were small, several sub-peaks were observed beside the main Bragg peak, suggesting interference domains in the surface region. The size of these domains was estimated to be about 500-nm using the semi-kinematical theory. After annealing at 1000°C, symmetric Bragg profiles without sub-peaks were observed, suggesting that the interference domains vanished during the annealing and uniform SOI layer was formed.

Although commercial electronic devices have already been fabricated on SOI substrates, a precise and quantitative strain evaluation of SOI layers has still not been done yet. Considering the more than ten-times difference in the thermal expansion coefficients between Si and SiO_2 at 1000°C, large strains should be formed at the interface during the fabrication processes, which degrade the crystalline quality of the SOI layers. Since x-ray-based techniques are non-destructive and have a large ability to obtain structural information in the layers, evaluating SOI substrates using x-ray reflectivity and grazing incidence x-ray diffraction is promising because they are sensitive to the surface and interface structures. Additionally, combining these techniques with oxidization instruments, one can observe the structural changes of the "real" interfaces instead of the quenched one, which also improve our understandings of the oxidization mechanism at the atomic-reaction level.

Acknowledgement

We thank the staff of the BL24XU beamline and Prof. Yasushi Kagoshima and Prof. Yoshiyuki Tsusaka of University of Hyogo for their support in our experiments. A part of this work was done with the approvals 2005A3102, 2005B3102, and 2006A3102 from the Japan Synchrotron Radiation Research Institute.

References

[1] J. Bardeen and W. H. Brattain, *Phys. Rev.*, **74**, 230-231 (1948)
[2] D. Kahng, *IEEE Trans. Electron Devices*, **ED-23**, 655-657, (1976).
[3] T. Takahagi, I. Nagai, A. Ishitani, H. Kuroda, and Y. Nagasawa, *J. Appl. Phys.*, **64**, 3516-3521 (1988).
[4] T. Takahagi, A. Ishitani, H. Kuroda, Y. Nagasawa, H. Ito, and S. Wakao, *J. Appl. Phys.*, **68**, 2187-2191 (1990).
[5] T. Aoyama, K. Goto, T. Yamazaki, and T. Ito, *J. Vac. Sci. Technol.*,**A14**, 2909-2915 (1996).
[6] T. Ohmi, M. Morita, A. Teramoto, K. Makihara, and K. S. Tseng, *Appl. Phys. Lett.*, **60**, 2126-2128 (1992).
[7] K. Izumi, Y. Omura, and S. Nakashima, *Electron. Lett.*, **22**, 775-777 (1986).
[8] M. Bruel, *Electron. Lett.*, **31**, 1201-1202 (1995)
[9] H. Omi, T. Kawamura, S. Fujikawa, Y. Tsusaka, Y. Kagoshima, J. Matsui, *Appl. Phys. Lett.*, **86**, 263112 (2005).
[10] B. E. Deal and A. S. Grove, *J. Appl. Phys.*, **36**, 3770-3778 (1965).
[11] H. Z. Massoud, J. D. Plummer, and E. A. Irene, *J. Electrochem. Soc.*, **132**, 1745-1753 (1985).
[12] J. Blanc, C. J. Buiocchi, M. S. Abrahams and W. E. Ham, *Appl. Phys. Lett.*, **30**, 120-122 (1977).
[13] F. J. Himpsel, F. R. McFeely, A. Taleb-Ibrahimi, J. A. Yarmoff and G. Hollinger, *Phys. Rev.*, **B38**,

6084-6096 (1988).
[14] K. Ohishi and T. Hattori, *Jpn. J. Appl. Phys.*, **33**, L675-678 (1994)
[15] Y. Sugita, S. Watanabe, N. Awaji and S. Komiya, *Appl. Surf. Sci.*, **100/101**, 268-271 (1997).
[16] S. Miyazaki, H. Nihsimura, M.Fukuda, L. Ley and J. Ristein, *Appl. Surf. Sci.*, **113/114**, 585-589 (1997).
[17] T. Watanabe and I. Ohdomari, *Appl. Surf. Sci,*, **162/163**, 116-121 (2000).
[18] D. A. Muller, T. Sorsh, S. Moccio, F. H. Bauman, K. Evans-Lutterodt and G. Tromp, *Nature*, 399, 758-761 (1999).
[19] T. Shimura, H. Misaki, I. Takahashi, and J. Harada, *J. Cryst. Growth*, **166**, 786-791, (1996).
[20] K. Tatsumura, T. Watanabe, D. Yamasaki, T. Shimura, M. Umeno, and I. Ohdomari, *Phys. Rev.*, **B 69**, 085212 (2004).
[21] J. M. Bloch, *J. Appl. Cryst.*, **18**, 33-36 (1985).
[22] T. Kawamura, Y. Watanabe, S. Fujikawa, K. Uchida, J. Matsui, Y. Kagoshima amd Y. Tsusaka, *J. Cryst. Growth*, **237-239**, 398-401 (2002).
[23] V.S. Speriosu, *J. Appl. Phys.*, **52**, 6094-6103 (1981).

(Received December 9, 2006;Accepted January 27, 2007)